



# $^{14}\text{N}$ break-up $\alpha$ emission with $^{59}\text{Co}$ , $^{93}\text{Nb}$ , and $^{197}\text{Au}$ targets at an incident energy of 250 MeV

C. Bhuptani<sup>1</sup> · D. Patel<sup>1</sup> · V. K. Ojha<sup>1</sup> · S. Mukherjee<sup>2</sup>

Received: 3 January 2024 / Accepted: 30 April 2024 / Published online: 23 May 2024  
© The Author(s) 2024

## Abstract

The emission of  $\alpha$  particles has been analyzed using a  $^{14}\text{N}$  projectile beam on  $^{59}\text{Co}$ ,  $^{93}\text{Nb}$ , and  $^{197}\text{Au}$  targets at an incident energy of 250 MeV, in the angular range from  $8^\circ$  to  $40^\circ$ . The estimated  $\alpha$  particles from the break-up channel and the pre-equilibrium mode were compared with the experimentally measured inclusive double differential cross sections at various angles at 250 MeV beam energy. The present results indicate that at such a high incident energy, a significant contribution to the  $\alpha$ -particle emission comes from direct reactions, which are dominant at forward angles. At larger emission angles, non-equilibrium and evaporation processes increase and compete with direct reactions.

**Keywords** Direct reactions ·  $\alpha$ -particle spectra · Heavy ion reaction · Break-up reactions · Serber model

## Introduction

At high incident energies of  $\sim 10$  MeV/A, the break-up analysis of tightly bound projectile nuclei is pivotal in shaping the resulting reaction dynamics and unravelling the mysteries of nuclear structure. In heavy ion nuclear reactions, the compound system processes compete with various direct processes. The major direct processes involve breaking up the incident projectile and/or the transfer of one or more nucleons between the projectile and the target nucleus [1]. The break-up reaction significantly affects the total cross section. The results of an experiment [2] showed that the fission reaction cross section is significantly less than the predicted one. The intricacies of the  $^{14}\text{N}$  break-up may illuminate its implications in nuclear physics.

The earlier studies of the reactions induced by  $^{12}\text{C}$  and  $^{14}\text{N}$ , revealed the production of large amounts of  $\alpha$  particles at  $\sim 10$  MeV/A incident energies. These  $\alpha$  particles

are primarily emitted in the forward direction, where their spectrum exhibits a broad peak with a mean energy roughly corresponding to the beam velocity. Further experiments have indicated that most of these  $\alpha$  particles originate from a projectile break-up [3–6]. The studies have shown that a significant fraction of the observed  $\alpha$  particles originates in the break-up of the projectile into an  $\alpha$ -particle and another fragment. One of these fragments may fuse with the target nucleus while the other fragment gets emitted almost undisturbed [7].

In the direct reaction, the projectile  $^{14}\text{N}$  may break into  $^{10}\text{B}$  and an  $\alpha$ -particle, or it may break into  $^{12}\text{C} + d$ , further the  $^{12}\text{C}$  break into  $^8\text{Be}$  and an  $\alpha$ -particle, thus producing three  $\alpha$  particles. Secondly,  $\alpha$  particles may get emitted after complete and incomplete fusion of the projectile with the target. Also, the contribution from evaporation channels should be considered. Thus, as mentioned above, the energy and angular distributions of the emitted  $\alpha$  particles from the different reaction channels would have different values.

At this energy, there is a contribution in the reaction cross section, mainly from a few reactions like: (1) An  $\alpha$ -particle produced during the projectile break-up. (2)  $\alpha$  particles emitted due to dissociation of another fragment. (3)  $\alpha$  particles being a participant fragment and re-emitted with reduced energy. (4) Pre-equilibrium  $\alpha$  particles emitted after complete and incomplete fusion. (5) Evaporated  $\alpha$  particles. In the past, the contribution of different reaction mechanisms was simulated as described in Ref. [7]. Recently, the

✉ D. Patel  
dipikapatel@phy.svnit.ac.in

✉ S. Mukherjee  
mukherjees@vut.cz

<sup>1</sup> Department of Physics, Sardar Vallabhbhai National Institute of Technology, Surat 395007, India

<sup>2</sup> Department of Electrical Power Engineering, Brno University of Technology, Technická 3058/10, 61600 Brno, Czech Republic

contribution of direct processes, pre-equilibrium emission, and evaporation of particles at such a high incident energy has been investigated in the interaction of  $^{14}\text{N}$  with  $^{59}\text{Co}$  and  $^{93}\text{Nb}$  at an incident energy of 250 MeV [8]. A modified PACE code employing Hauser–Feshbach formalism was utilized to calculate emitted  $\alpha$  particles cross sections. The modified PACE code takes into account equilibrium and pre-equilibrium processes. More details on the theoretical approach are given in Ref. [9].

In the present work, we have adopted the analysis method described in Ref. [10]. The internal momentum of the  $\alpha$ -particle is derived from a Yukawa-type wave function that gives the correct separation energy of  $\alpha$ -particle from the  $^{14}\text{N}$ . The primary object of this work is to explore the  $^{14}\text{N}$  break-up  $\alpha$  contribution using  $^{59}\text{Co}$ ,  $^{93}\text{Nb}$ , and  $^{197}\text{Au}$  targets. In the present break-up study, an  $\alpha$  cluster structure of  $\alpha + ^{10}\text{B}$  is considered for  $^{14}\text{N}$  nucleus.

The contribution from pre-equilibrium emission and evaporation of particles in the experimentally measured  $\alpha$  particle cross sections was already investigated using the same projectile  $^{14}\text{N}$  elsewhere [8]. Therefore, unfolding the  $^{14}\text{N}$  break-up contributions involving medium weight to heavy target masses and comparing them with other possible reaction channels would be interesting.

## Experimental details

The experiment was performed at the iThemba LABS, Somerset West, South Africa cyclotron facility. Experimental data were measured for the interaction of  $^{14}\text{N}$  with  $^{197}\text{Au}$  target at an incident energy of 250 MeV. Data were acquired at various scattering angles ranging from  $8^\circ$  to  $40^\circ$  following the method similar to the one for  $^{14}\text{N} + ^{59}\text{Co}$ ,  $^{93}\text{Nb}$  systems [8]. More details of the detector arrangement and electronics used in the experiment are described in Ref. [7], and further details of the facility are provided in Ref. [11]. The experimentally measured double differential cross sections for  $\alpha$  particles are shown in Figs. 1, 2, 3, 4, 5.

## Theoretical method

We used the Serber approximation [10, 12] to calculate the  $^{14}\text{N}$  break-up into  $\alpha$  particle and  $^{10}\text{B}$  fragments. We have considered  $\alpha$  and  $^{10}\text{B}$  as spectator and participant fragments, respectively. In this method, the target nucleus plays no role except for the projectile break-up at the collision. The momentum of the emitted  $\alpha$ -particle is ( $p_\alpha$ ) the sum of the momentum due to the center of mass motion of the incident  $^{14}\text{N}$  ( $p_N$ ) and the momentum due to the internal motion of  $\alpha$ -particle in the  $^{14}\text{N}$  at the time of break up ( $p$ ), that is,  $p_\alpha = \frac{2}{7}p_N + p$ . Also, according to this, approximation, the break-up transition matrix is given by the Fourier transform

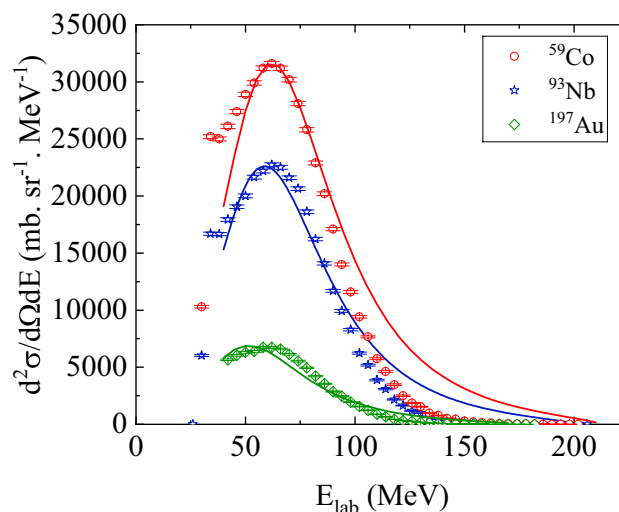


**Fig. 1** (Colour Online) Experimental (open symbols) and calculated (solid curve) energy Spectra of  $\alpha$  particles measured at  $8^\circ$  for  $^{14}\text{N}$  with  $^{59}\text{Co}$  (red circles),  $^{93}\text{Nb}$  (blue stars) and  $^{197}\text{Au}$  (green diamonds) at 250

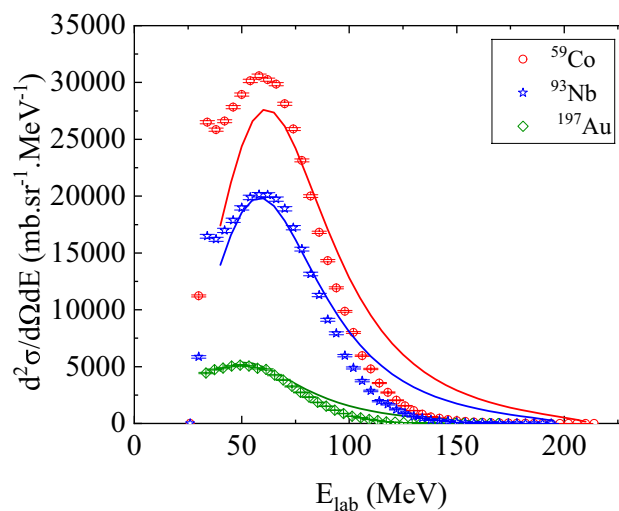


**Fig. 2** (Colour Online) Experimental (open symbols) and calculated (solid curve) energy Spectra of  $\alpha$  particles measured at  $10^\circ$  for  $^{14}\text{N}$  with  $^{59}\text{Co}$  (red circles),  $^{93}\text{Nb}$  (blue stars) and  $^{197}\text{Au}$  (green diamonds) at 250 MeV

of the function describing the relative motion of  $\alpha$ -particle and  $^{10}\text{B}$  fragment in  $^{14}\text{N}$ . The square of the transition matrix is provided by,

$$|T|^2 \propto \left| \Psi \left( p_\alpha - \frac{2}{7} p_N \right) \right|^2 \quad (1)$$

where

$$\Psi(p) = \frac{1}{(2\pi\hbar)^{3/2}} \int \Psi(r) \exp \left( -\frac{i}{\hbar} (p \cdot r) \right) d^3 r \quad (2)$$

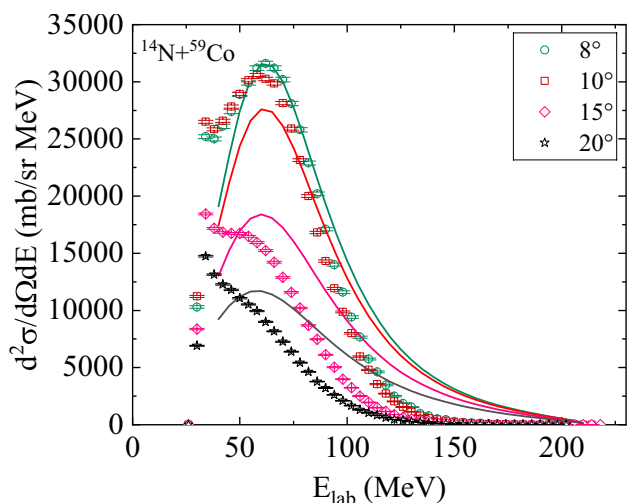


**Fig. 3** (Colour Online) Experimental (open symbols) and calculated (solid curve) energy Spectra of  $\alpha$  particles measured at  $8^\circ$  (green circles),  $10^\circ$  (red squares),  $15^\circ$  (pink diamonds) and  $20^\circ$  (black stars), for  $^{14}\text{N}$  with  $^{59}\text{Co}$  at 250 MeV

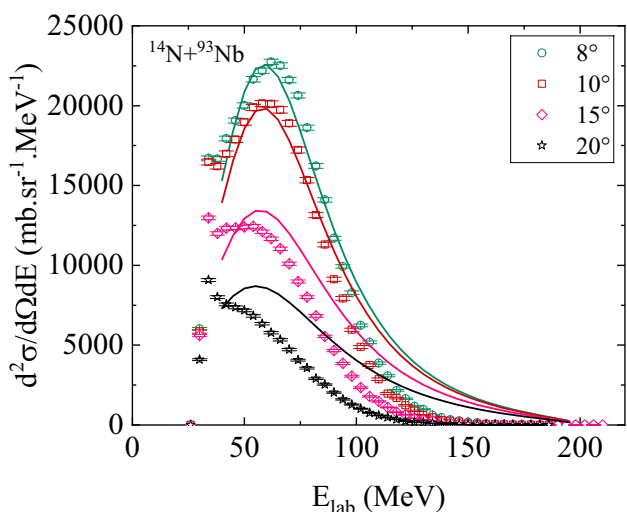


**Fig. 4** (Colour Online) Experimental (open symbols) and calculated (solid curve) energy Spectra of  $\alpha$  particles measured at  $8^\circ$  (green circles),  $10^\circ$  (red squares),  $15^\circ$  (pink diamonds) and  $20^\circ$  (black stars), for  $^{14}\text{N}$  with  $^{93}\text{Nb}$  at an incident energy of 250 MeV

is the Fourier transform of the wave function.

$$\Psi(r) = C \left( \frac{\alpha}{2\pi} \right)^{\frac{1}{2}} \frac{1}{r} \exp(-\alpha.r) \tag{3}$$

Here,

$$\alpha = \frac{(2\mu\epsilon)^{\frac{1}{2}}}{2\pi\hbar} \tag{4}$$

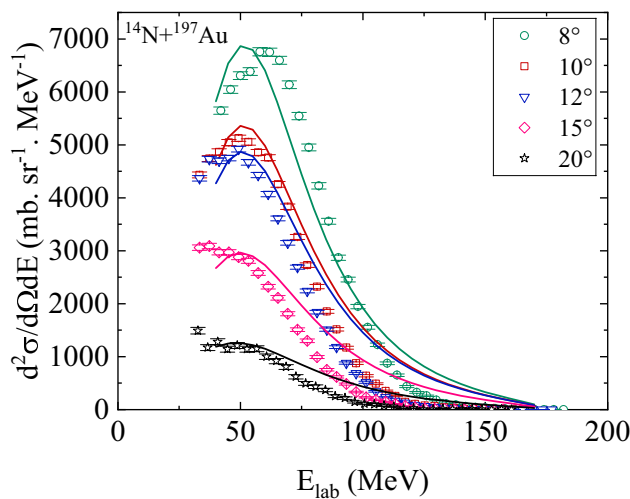


**Fig. 5** (Colour Online) Experimental (open symbols) and calculated (solid curve) energy Spectra of  $\alpha$  particles measured at  $8^\circ$  (green circles),  $10^\circ$  (red squares),  $12^\circ$  (blue down-triangle),  $15^\circ$  (pink diamonds) and  $20^\circ$  (black stars), for  $^{14}\text{N}$  with  $^{197}\text{Au}$  at 250 MeV

and  $C$  is the normalization constant,  $\mu$  is reduced mass, and  $\epsilon$  is the binding energy of  $\alpha$ -particle in  $^{14}\text{N}$ , which is 11.61 MeV. So, the obtained transition matrix is given as

$$|T|^2 \propto \frac{1}{\pi^2} \frac{(2\mu\epsilon)^{\frac{1}{2}}}{\left[ (2\mu\epsilon + \left( \frac{2}{7}p_N - p_\alpha \right)^2)^2 \right]} \tag{5}$$

The energy distribution of  $\alpha$  particles is given by multiplying the transition matrix by the three-body phase space factor [13, 14]. When the target mass number  $A$  becomes  $\frac{1}{3}A \gg 1$  then Eq. (5) is reduced to the expression.

$$\frac{d^2\sigma}{d\Omega dE} \propto \frac{4}{\pi} m_\alpha m_B \frac{p_\alpha p_B (2\mu\epsilon)^{\frac{1}{2}}}{\left[ (2\mu\epsilon + \left( \frac{2}{7}p_N - p_\alpha \right)^2)^2 \right]} \tag{6}$$

where  $m_\alpha$  and  $m_B$  are the masses of  $\alpha$ -particle and  $^{10}\text{B}$ , and  $p_\alpha, p_B, p_N$  are the momentum of the  $\alpha$ -particle,  $^{10}\text{B}$ , and  $^{14}\text{N}$ , respectively. The  $|T|^2$  term mainly determines the energy spectrum and is only slightly changed by the phase space factor. The peak energy and the FWHM of the bump spectra deduced from the  $|T|^2$  term only is about  $\frac{m_\alpha}{m_p} E_N$  and  $1.21 \sqrt{E_N \epsilon}$  respectively, at forward angles, which agree with the experimental results.

### Results and discussion

The energy spectra of the  $\alpha$  particles emitted from the break-up of  $^{14}\text{N}$  at the collision with  $^{59}\text{Co}$ ,  $^{93}\text{Nb}$  and  $^{197}\text{Au}$  targets at 250 MeV have been examined. Our analysis includes

investigating  $\alpha + {}^{10}\text{B}$  cluster structure for breaking up  ${}^{14}\text{N}$  projectile nucleus at various angles, using the Serber Model. The experimentally measured double differential cross section of  $\alpha$  particles at different angles is compared with the present results on break-up calculations. Figures 1 and 2 illustrate the measured energy spectra of emitted  $\alpha$  particles at  $8^\circ$  and  $10^\circ$ , respectively, in comparison with the corresponding break-up calculations, for reactions involving  ${}^{14}\text{N}$  with  ${}^{59}\text{Co}$ ,  ${}^{93}\text{Nb}$ , and  ${}^{197}\text{Au}$  at an incident energy of 250 MeV. Remarkably, at smaller angles, the reaction cross section remains relatively constant. Furthermore, a conspicuous, broad peak is observed in the energy spectrum, centered around  $\frac{2}{7}E_N \sim 70\text{MeV}$ . This peak corresponds to  $\alpha$  particles originating from incomplete fusion and pre-equilibrium emission. An extended tail is visible, attributed to spectator  $\alpha$  particles originating from the direct break-up process.

In the present method, the experimental data were not fitted using any free parameters or distribution models throughout the entire study, except for incorporating a normalization constant. The identical normalization constant was applied across various angles to calculate the break-up cross sections for the specific target under investigation [12]. Direct break-up reactions are predominant at very forward angles. Hence, the normalization constant was chosen to align with measurements at  $8^\circ$ , ensuring uniformity across all angles. There is a notable correspondence between the present calculations and experimental results for all systems, including  ${}^{59}\text{Co}$ ,  ${}^{93}\text{Nb}$ , and  ${}^{197}\text{Au}$  at both  $8^\circ$  and  $10^\circ$ . However, for the medium weight target nucleus  ${}^{59}\text{Co}$  at  $10^\circ$ , the present calculations underestimate the cross sections, possibly because the same normalization constant was used for both  $8^\circ$  and  $10^\circ$ .

Figures 3, 4, 5 show the measured energy spectra of emitted  $\alpha$  particles along with the results of break-up calculations

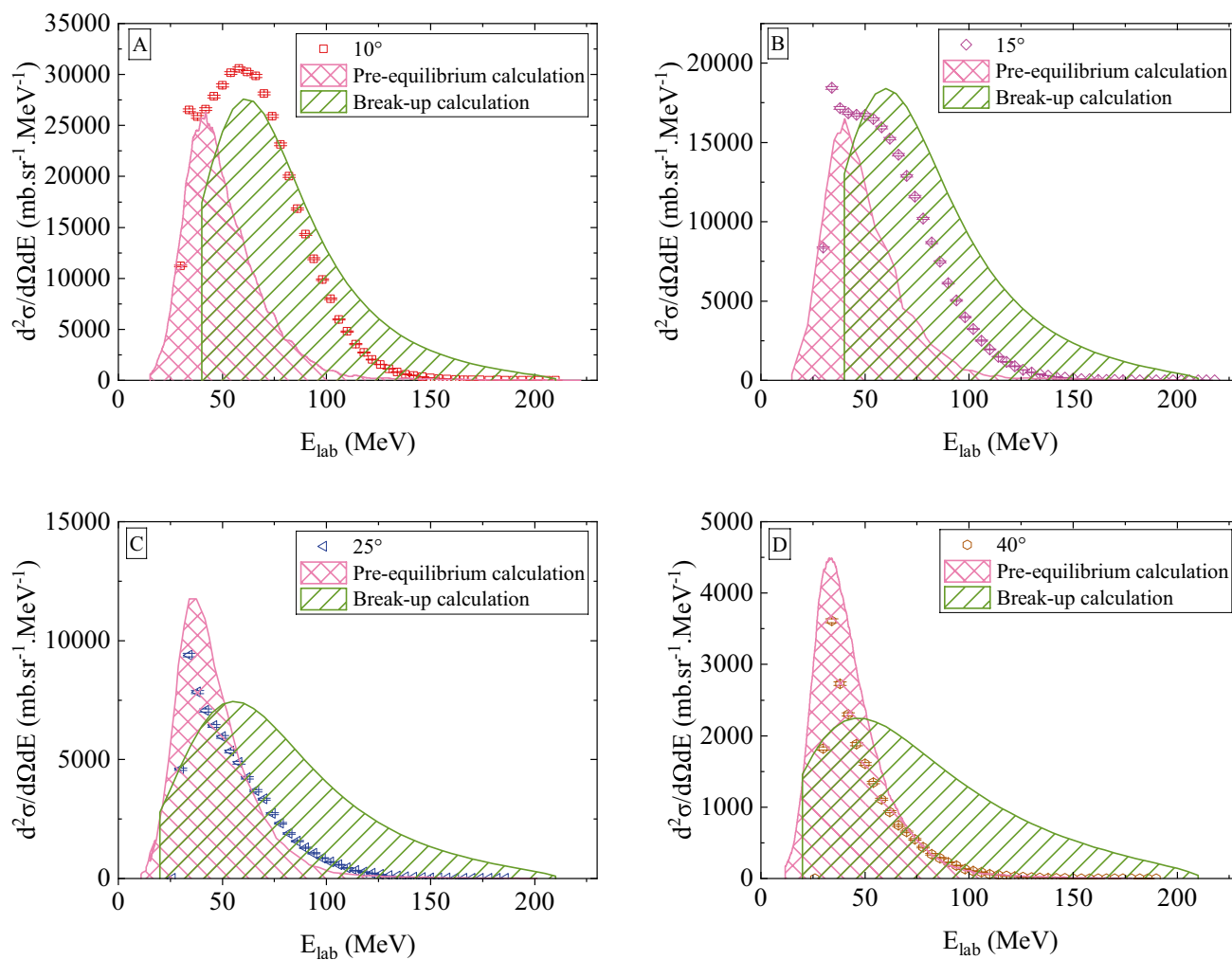


**Fig. 6** (Colour Online) The  $\alpha$  particles energy spectra at angles  $10^\circ$  (red squares) **A**,  $15^\circ$  (pink diamonds) **B**,  $25^\circ$  (blue left-triangle) **C**, and  $40^\circ$  (brown hexagon) **D**, for  ${}^{14}\text{N}$  with  ${}^{59}\text{Co}$  at 250 MeV. The filled

curve (green) shows the break-up calculation, and the filled curve (pink) shows the contribution of pre-equilibrium  $\alpha$  particles

at various angles for  $^{14}\text{N}$  with  $^{59}\text{Co}$ ,  $^{93}\text{Nb}$  and  $^{197}\text{Au}$ . The figures clearly indicate that as we move towards more backward angles, the peak gradually diminishes, vanishing entirely after  $20^\circ$ .

Figures 6 and 7 compare measured double differential cross sections with the calculated break-up and pre-equilibrium  $\alpha$  particles contributions [8]. These comparisons aim to understand the behaviour of emitted  $\alpha$  particles during the reaction across various angles. It is evident that at forward angles ( $8^\circ$ – $15^\circ$ ), direct reactions dominate and closely match break-up calculations. However, deviations between the calculated break-up spectra and experimental data become apparent as the scattering angle increases towards larger or backward angles ( $25^\circ$ – $40^\circ$ ), where the non-break-up channels such as pre-equilibrium and equilibrium processes come into play and align more closely with pre-equilibrium calculations. This discrepancy is attributed to the presence and contribution of other reaction channels.

## Conclusion

$^{14}\text{N}$  break-up  $\alpha$  contributions have been studied at various angles using  $^{59}\text{Co}$ ,  $^{93}\text{Nb}$  and  $^{197}\text{Au}$  targets at an incident energy of 250 MeV. The present work focused on calculating the  $^{14}\text{N}$  breaking up into an  $\alpha$ -particle and  $^{10}\text{B}$  nucleus utilizing the Serber model's asymptotic wave function. The experimentally measured double differential cross section of  $\alpha$  particles at various angles is compared with the current results obtained from break-up calculations. The results of these calculations exhibit good agreement with available experimentally measured data, offering a clear explanation for the substantial  $\alpha$ -particle yields resulting from the break-up of  $^{14}\text{N}$  and also reflecting the difference in their origins. As the incident energy increases, the projectile becomes less efficient in transferring the kinetic energy to the target in thermal energy. To account for this intriguing experimental observation, it has become

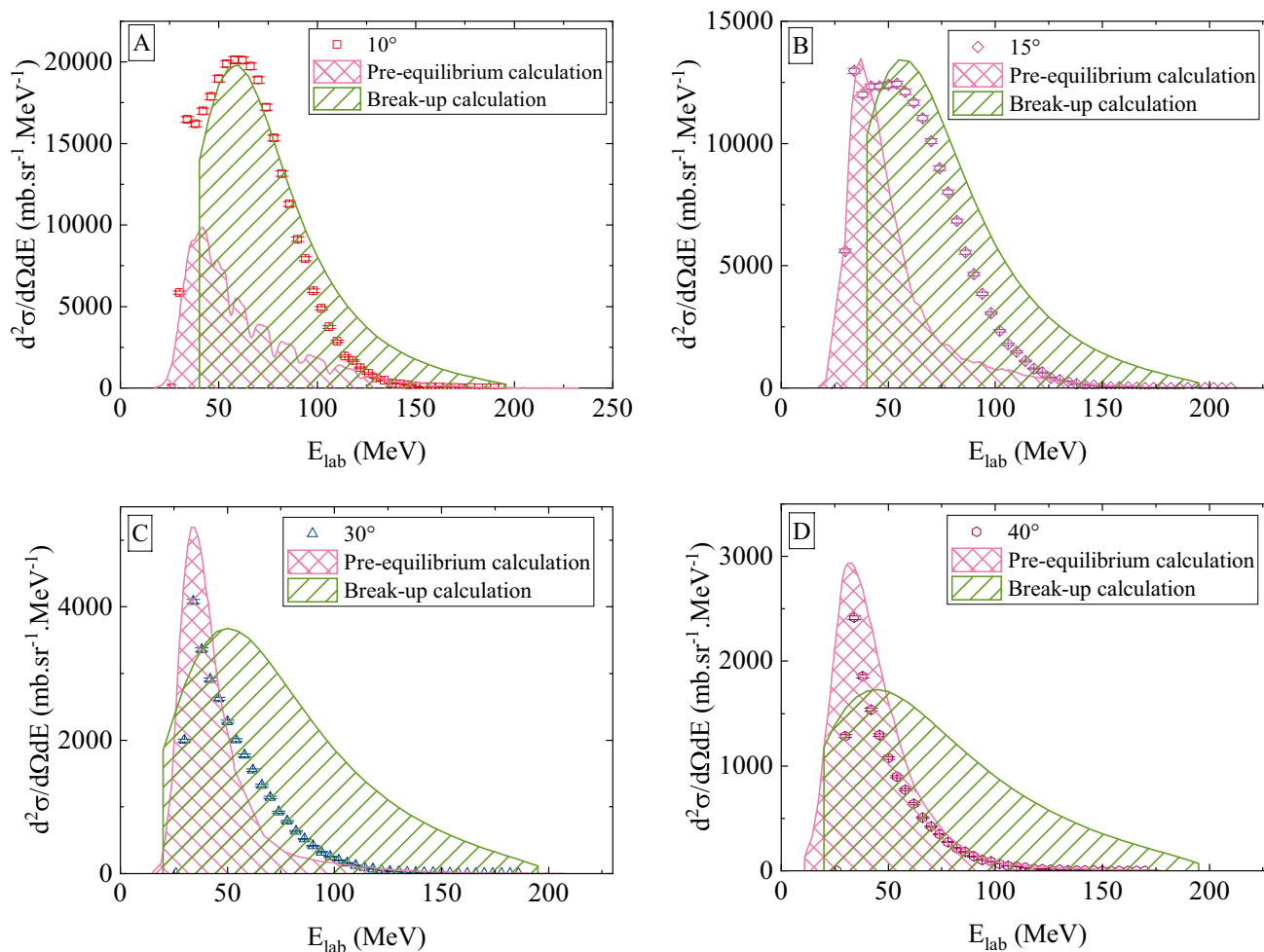


**Fig. 7** (Colour Online) The  $\alpha$  particles energy spectra at angles  $10^\circ$  (red squares) **A**,  $15^\circ$  (pink diamonds) **B**,  $30^\circ$  (indigo triangles) **C**, and  $40^\circ$  (brown hexagon) **D**, for  $^{14}\text{N}$  with  $^{93}\text{Nb}$  at 250 MeV. The filled

curve (green) shows the break-up calculation, and the filled curve (pink) shows the contribution of pre-equilibrium  $\alpha$  particles

necessary to postulate not only the growing significance of incomplete fusion reactions at higher incident energies but also that the rapid dissipation of energy imparted to the  $^{14}\text{N}$  nucleus will not warm the nuclei and lead this reaction to the pre-equilibrium emission of  $\alpha$  particles. Break-up calculations based on the  $\alpha$ -particle momentum distribution derived from the asymptotic relative wave function of successfully replicate peak energies in the analyzed energy range. Figs. 6 and 7 visually demonstrate the contributions from incomplete fusion, complete fusion, and pre-equilibrium emission of  $\alpha$  particles, particularly emphasizing the significance of projectile break-up at very forward angles. However, the Serber model falls short in providing information regarding excited state or resonant break-up phenomena. Furthermore, the model confines us to direct break-up within the target field, neglecting other possible reaction pathways. Hence, for more accurate and comprehensive results, employing DWBA (Distorted Wave Born Approximation) can yield more reliable outcomes [10].

**Acknowledgements** The authors thank Prof. J. J. Lawrie and his research group, as well as the entire staff of iThemba LABS, South Africa, for their help in smooth completion of the experiment. D. Patel acknowledges financial support through the Seed Money Research grant at S.V.N.I.T, DoP (Project No.: 2021-22/DoP/03). S. Mukherjee thanks Brno University of Technology, for his appointment as Visiting Professor.

**Funding** Open access publishing supported by the National Technical Library in Prague.

**Open Access** This article is licensed under a Creative Commons Attribution 4.0 International License, which permits use, sharing, adaptation, distribution and reproduction in any medium or format, as long as you give appropriate credit to the original author(s) and the source, provide a link to the Creative Commons licence, and indicate if changes were made. The images or other third party material in this article are included in the article's Creative Commons licence, unless indicated otherwise in a credit line to the material. If material is not included in the article's Creative Commons licence and your intended use is not permitted by statutory regulation or exceeds the permitted use, you will need to obtain permission directly from the copyright holder. To view a copy of this licence, visit <http://creativecommons.org/licenses/by/4.0/>.

## References

1. Britt HC, Quinton AR (1961)  $\alpha$  Particles and protons emitted in the bombardment of  $^{197}\text{Au}$  and  $^{209}\text{Bi}$  by  $^{12}\text{C}$ ,  $^{14}\text{N}$ , and  $^{16}\text{O}$  projectiles. *Phys Rev* 124(3):877–887
2. Gordon GE, Larsh AE, Sikkeland T, Seaborg GT (1960) Fission of gold by carbon ions. *Phys Rev* 120(4):1341–1348
3. Gadioli E, Birattari C, Cavinato M, Fabrici E, Erba EG, Allori V et al (1997) Comprehensive study of the reactions induced by  $^{12}\text{C}$  on  $^{103}\text{Rh}$  up to 33 MeV/nucleon. *Phys Lett B* 394(1):29–36
4. Parker DJ, Vergani P, Gadioli E, Hogan JJ, Vettore F, Gadioli-Erba E et al (1991) Recoil range study of complete and incomplete fusion of C with Au at 10 MeV/nucleon. *Phys Rev C* 44(4):1528–1540
5. Vergani P, Gadioli E, Vaciago E, Fabrici E, Gadioli Erba E, Galmarini M et al (1993) Complete and incomplete fusion and emission of preequilibrium nucleons in the interaction of  $^{12}\text{C}$  with  $^{197}\text{Au}$  below 10 MeV/nucleon. *Phys Rev C* 48(4):1815–1827
6. Gadioli E, Birattari C, Cavinato M, Fabrici E, Gadioli Erba E, Allori V et al (1998) Angular distributions and forward recoil range distributions of residues created in the interaction of  $^{12}\text{C}$  and  $^{16}\text{O}$  ions with  $^{103}\text{Rh}$ . *Nucl Phys A* 641(3):271–296
7. Gadioli E, Cavinato M, Fabrici E, Gadioli Erba E, Birattari C, Mica I et al (1999) Alpha particle emission in the interaction of  $^{12}\text{C}$  with  $^{59}\text{Co}$  and  $^{93}\text{Nb}$  at incident energies of 300 and 400 MeV. *Nucl Phys A* 654(3–4):523–540
8. Acharya J, Mukherjee S, Steyn GF, Förtsch SV, Smit FD, Newman RT et al (2020) Non-equilibrium emission of alpha particles in the interaction of  $^{14}\text{N}$  with  $^{59}\text{Co}$  and  $^{93}\text{Nb}$  at incident energy of 250 MeV. *Nucl Phys A* 996:121695
9. Fotina OV, Eremenko DO, Parfenova YL, Platonov SY, Yuminov OA, Kravchuk VL et al (2010) Pre-equilibrium effects in the secondary particle spectra in the reactions with heavy ions. *Int J Mod Phys E* 19(5–6):1134–1140
10. Matsuoka N, Shimizu A, Hosono K, Saito T, Kondo M, Sakaguchi H et al (1978) Projectile break-up and the continuum spectra of the ( $^3\text{He}$ , d) reaction. *Nucl Phys A* 311(1–2):173–187
11. Pilcher JV, Cowley AA, Whittal DM, Lawrie JJ (1989) Protons of 200 MeV incident on  $^{12}\text{C}$ . I. Coincident proton emission from the continuum. *Phys Rev C* 40(5):1937–1949
12. Serber R (1947) The production of high energy neutrons by stripping. *Phys Rev* 72(11):1008–1016
13. Block MM (1956) Phase-space integrals for multiparticle systems. *Phys Rev* 101(2):796–799
14. Skjeggstad O (1964) Notes on phase space. <http://cds.cern.ch/record/864958>

**Publisher's Note** Springer Nature remains neutral with regard to jurisdictional claims in published maps and institutional affiliations.